

ICONN 2015 [4<sup>th</sup> -6<sup>th</sup> Feb 2015]  
International Conference on Nanoscience and Nanotechnology-2015  
SRM University, Chennai, India

## Spectral analysis of europium doped Borate Zinc Magnesium glass

M. Venkateswarlu\* and B.H. Rudramadevi

Department of Physics, Sri Venkateswara University, Tirupati-517502, India

**Abstract :** Borate Zinc Magnesium glasses doped with (0.2%)  $\text{Eu}^{3+}$  ions (labelled as  $\text{Eu}^{3+}$ :BZM) have been prepared by rapid melt quenching technique. The obtained glass is circular design displaying bright *red colour* under an UV source, and characterized for their luminescence behavior through various spectroscopic techniques such as absorption, excitation, emission and decay profiles at room temperature. Five absorption peaks of  $\text{Eu}^{3+}$  ion were observed due to transitions from ground state to different excited states in 300–2300 nm region. From the emission spectrum of  $\text{Eu}^{3+}$ :BZM glass, five emission transitions have been observed at 579 nm, 591 nm, 613 nm, 652 nm, and 701 nm and are assigned to their electronic transitions  ${}^5\text{D}_0 \rightarrow {}^7\text{F}_0, {}^7\text{F}_1, {}^7\text{F}_2, {}^7\text{F}_3$  and  ${}^7\text{F}_4$  respectively, with  $\lambda_{\text{exci}} = 393 \text{ nm}$  ( ${}^7\text{F}_0 \rightarrow {}^5\text{L}_6$ ). The transition  ${}^5\text{D}_0 \rightarrow {}^7\text{F}_2$  which is centered at 613 nm has been known as a hypersensitive emission which obeys the selection rule of  $\Delta J = 2$  resulting in a strong and intense *red* emission. For such a prominent visible colour emitting glass, emission transition (613 nm) decay curve has also been measured in evaluating emission band lifetime (1.81 ms) and the emission process that arise in the glass has been explained in terms of energy level diagram.

**Keywords:**  $\text{Eu}^{3+}$  doped glasses - spectral analysis.

### Introduction

Glasses doped with rare earth (RE) ions have emerged as a significant category of solid state luminescent material and are finding ever-increasing applications as compact visible and NIR lasers, broad band amplifiers, light-emitting devices, color display panels, optical data storage, sensors, optical communications, etc<sup>1,2,3</sup>. In particular, the rising demand in visible laser sources has provoked significant exploitation of RE ions like  $\text{Eu}^{3+}$ ,  $\text{Sm}^{3+}$ ,  $\text{Dy}^{3+}$ ,  $\text{Tm}^{3+}$  and  $\text{Pr}^{3+}$  within various disordered matrices<sup>1,2,4</sup>. Within the rare earth family, trivalent europium ( $\text{Eu}^{3+}$ ) is an important activator for inorganic lattices and is well recognized as a powerful pure red light-emitting center for display devices due to its dominant  ${}^5\text{D}_0 \rightarrow {}^7\text{F}_2$  electronic transition<sup>2,4,5,6,7,8,9,10,11,12</sup>. The role of the disordered glass environment on the optical properties of rare earth ions is significantly important because it influences the intra-configurational optical transitions. The non-degenerate nature of the (excited)  ${}^5\text{D}_0$  and the  ${}^7\text{F}_0$  (ground) state and relatively simple energy level system makes  $\text{Eu}^{3+}$  ions a highly convenient spectroscopic probe for studying the symmetry and inhomogeneity (crystal field effect) present in the host matrices and consequently present valuable information regarding structure and bonding properties of various hosts<sup>13,14</sup>. In a free  $\text{Eu}^{3+}$  ion the transitions between the different levels of the  $4f^7$  configuration are prohibited by the Laporte selection rule<sup>15</sup>. However, when the  $\text{Eu}^{3+}$  ions are embedded within a matrix (glass), the ligand field due to the surrounding ions constituting the host perturbs the free ion

levels, causing admixing of energy states of different configurations (e.g.  $4f^n$  and  $4f^{n-1}d^1$ , etc.) resulting in non-degeneracy so that the intra-configurational ( $4f^n$ ) transitions become allowed<sup>16</sup>. Slight disparity in the bonding parameters (e.g. ligand distance, ligand angle, coordination number and covalency) causes variation in the strength of the ligand field and consequently in the energy levels of the free ion. Thus, the rare earth absorption and fluorescence spectra are governed by the local environment around the RE ion.

A host of borate rich glasses containing alkaline earth oxides along with ZnO, PbO, TeO<sub>2</sub> and Bi<sub>2</sub>O<sub>3</sub> as glass modifiers are optimistic materials for their probable applications in the fields of optical communications (optical fibers), laser hosts, optical filters,  $\gamma$ -ray absorbers, photonic devices etc. The metal oxides ZnO, TeO<sub>2</sub>, PbO and Bi<sub>2</sub>O<sub>3</sub> etc are well known conditional glass modifiers. Glasses containing these metal oxides give rise to good non-linear optical properties. The metal oxides like PbO, ZnO behave as glass network formers (GNF) and also as glass network modifiers (GNM). The alkaline earth oxides MgO, CaO, SrO and BaO improve the glass forming nature, they can also take the positions of GNF and GNM in glass matrix.

Keeping in view the applications of alkaline earth borate glasses containing heavy metal oxides, the present work has been undertaken to study both absorption and photoluminescence spectra properties of Eu<sup>3+</sup> ( $4f^6$ ) ions doped in B<sub>2</sub>O<sub>3</sub>-ZnO-MgO glass.

## 2. Experimental Studies

### 2.1 Glasses preparation

Glasses studied in the present work were prepared by a standard melt quenching technique. The chemical compositions (all are in mol %) of the host glass with and without rare earth ions as dopants are as follows:

- (i) 65B<sub>2</sub>O<sub>3</sub>-20ZnO-15MgO (host BZM glass)
- (ii) 64.8B<sub>2</sub>O<sub>3</sub>-20ZnO-15MgO-0.2Eu<sub>2</sub>O<sub>3</sub> (Eu<sup>3+</sup>: BZM glass)

The chemicals used were reagent grade H<sub>3</sub>BO<sub>3</sub>, ZnCO<sub>3</sub>, MgCO<sub>3</sub> and Eu<sub>2</sub>O<sub>3</sub>. All these chemicals were weighted separately in 10 g each batch, thoroughly mixed and finely powdered using agate mortar and pestle. Each batch of chemical mix was transferred into porcelain crucible and each of those was sintered in an electric furnace for an hour at 980 ° each batch separately. Those melts were quenched in between two smooth surfaced brass plates to obtain circular glass discs of 2-3 cm in diameter with 0.3 cm in thickness. The host BZM glass was transparent and colourless, Eu<sup>3+</sup>: BZM glass did exhibit a *red* emission under an UV source. **Fig. 1** displays the glasses developed in the present work

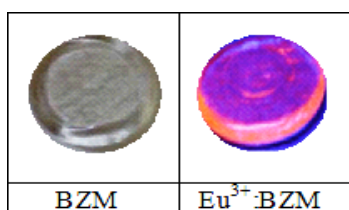


**Fig. 1.** Display of host (BZM) glass, Eu<sup>3+</sup> (0.2 mol %) ions doped BZM glasses.

### 2.2 Measurements

The optical absorption spectrum of Eu<sup>3+</sup> glass was measured on a Varian-Cary Win spectrometer (JASCO V-570). The excitation and emission spectra were obtained on a SPEX Fluorolog-2 Fluorimeter (Model-II) with Data max software to acquire the data with Xe-flash lamp (150W) as the excitation source. A Xe-flash lamp with a phosphorimeter attachment was used to measure the lifetimes of the emission transitions of Eu<sup>3+</sup> glass.

## 3. Results and discussion

The VIS and NIR optical absorption spectrum of 0.2mol% Eu<sup>3+</sup> doped BZM glass is shown in **Fig.2**, with five absorption bands such as  $^7F_0 \rightarrow ^5L_6$  (394 nm),  $^7F_0 \rightarrow ^5D_2$  (463 nm),  $^7F_0 \rightarrow ^5D_1$  (526 nm),  $^7F_0 \rightarrow ^7F_6$  (2094 nm) and  $^7F_1 \rightarrow ^7F_6$  (2205 nm). The assignments have been made following by published articles<sup>17,18</sup>. The

${}^7F_7 \leftrightarrow {}^5D_7$  absorption and emission bands are spin forbidden and hence they are very weak<sup>19</sup>. The close examination of band positions ( ${}^7F_0 \rightarrow {}^7F_6$ ,  ${}^7F_1 \rightarrow {}^7F_6$ ) reveals that the energy gap between  ${}^7F_0$  and  ${}^7F_1$  levels is  $\sim 240 \text{ cm}^{-1}$  which is comparable to other  $\text{Eu}^{3+}$  doped glasses<sup>18</sup>.

**Fig. 3** shows the excitation spectrum of the 0.2 mol %  $\text{Eu}^{3+}$ : BZM glass, monitoring emission at 613 nm, which corresponds to the  ${}^5D_0 \rightarrow {}^7F_2$  transition. From this spectrum, six excitation bands which could be assigned to the electronic transitions of  ${}^7F_0 \rightarrow {}^5D_4$  at 360 nm,  ${}^7F_0 \rightarrow {}^5L_7$  at 380 nm,  ${}^7F_0 \rightarrow {}^5L_6$  at 393 nm,  ${}^7F_0 \rightarrow {}^5D_3$  at 413 nm,  ${}^7F_0 \rightarrow {}^5D_2$  at 463 nm and  ${}^7F_0 \rightarrow {}^5D_1$  at 532 nm are identified. Among these, the prominent excitation band  ${}^7F_0 \rightarrow {}^5L_6$  at 393 nm has been chosen to measure the emission spectrum of  $\text{Eu}^{3+}$ : BZM glass.

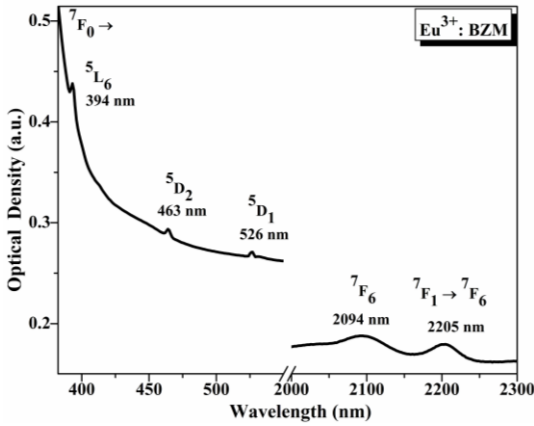


**Fig. 2.** VIS-NIR absorption spectrum of (0.2 mol %)  $\text{Eu}^{3+}$ : BZM glass

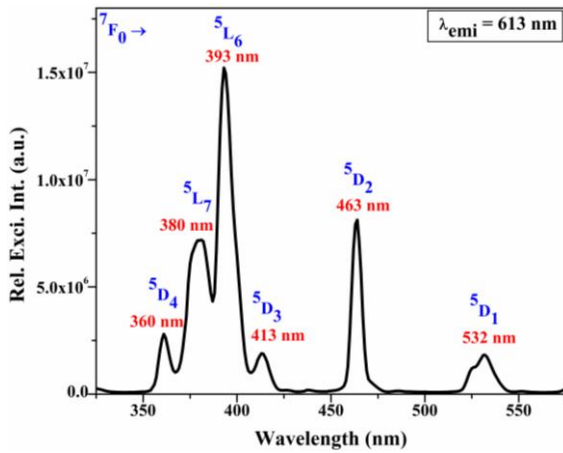


**Fig. 3.** Excitation spectrum of (0.2 mol %)  $\text{Eu}^{3+}$ : BZM glass

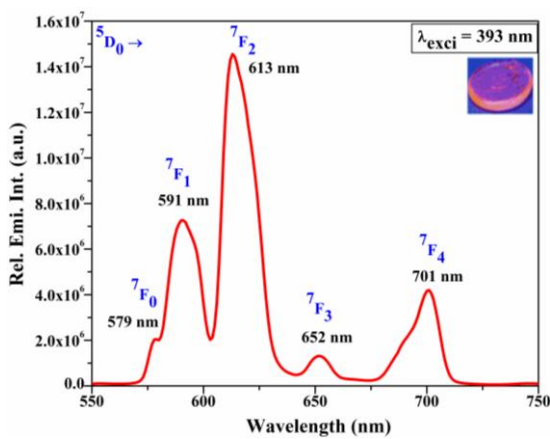


**Fig. 4.** Emission spectrum of (0.2 mol %)  $\text{Eu}^{3+}$ : BZM glass

**Fig. 4** shows emission spectrum of  $\text{Eu}^{3+}$ : BZM glass, with five emission transitions of  ${}^5\text{D}_0 \rightarrow {}^7\text{F}_0$  (579 nm),  ${}^5\text{D}_0 \rightarrow {}^7\text{F}_1$  (591 nm),  ${}^5\text{D}_0 \rightarrow {}^7\text{F}_2$  (613 nm),  ${}^5\text{D}_0 \rightarrow {}^7\text{F}_3$  (652 nm) and  ${}^5\text{D}_0 \rightarrow {}^7\text{F}_4$  (701 nm) as was reported previously in literature<sup>17</sup>. Of these transitions,  ${}^5\text{D}_0 \rightarrow {}^7\text{F}_2$  (613 nm) could be found to be *bright red* emission transition. In  $\text{Eu}^{3+}$ , due to the shielding effect of  $4f^6$  electrons (by 5s and 5p electrons) in the outer shell sharp and narrow emission peaks could thus be observed.

From the measured emission spectrum, it is noticed that the emissions from  ${}^5\text{D}_0$  state are present whereas from excited states  ${}^5\text{D}_{j(=1, 2 \& 3)}$  could not be measured thus indicating a fact that  ${}^5\text{D}_0$  state has a long lifetime. The absence of emissions from  ${}^5\text{D}_{j(=1, 2 \& 3)}$  states, could also be due the existence of higher energy phonons in the glasses, i.e. when  $\text{Eu}^{3+}$  ions are excited to any level above the  ${}^5\text{D}_0$  there is a fast non-radiative multiphonon relaxation to this level and the emission from the  ${}^5\text{D}_{j(=1, 2 \& 3)} \rightarrow {}^7\text{F}_j$  are several orders smaller than  ${}^5\text{D}_0 \rightarrow {}^7\text{F}_j$ , so the emission from these three transitions cannot be observed<sup>20</sup>. The intense bands in the range 550 nm–750 nm are caused by the  ${}^5\text{D}_0 \rightarrow {}^7\text{F}_{j(=1, 2, 3, 4)}$  could be due to high non-radiative relaxations from the excited states of energy higher than  ${}^5\text{D}_0$  state. A weak emission peak observed at 579 nm is assigned to  ${}^5\text{D}_0 \rightarrow {}^7\text{F}_0$  electric dipole transition. According to parity selection rule  $\Delta J = 0$ ,  ${}^5\text{D}_0 \rightarrow {}^7\text{F}_0$  transition is forbidden (as the transition from  $J = 0 \rightarrow 0$  is forbidden) when  $\text{Eu}^{3+}$  ion occupies an inversion symmetry (Centro-symmetric) environment in the crystal lattice field. This transition is very sensitive to the local environment of  $\text{Eu}^{3+}$ . If  $\text{Eu}^{3+}$  occupies non-inversion symmetry environments with local symmetries of  $C_n$ ,  $C_{nv}$  or  $C_s$ , then the transition  ${}^5\text{D}_0 \rightarrow {}^7\text{F}_0$  is not strictly forbidden and can give rise to weak lines in the emission spectra. Generally, the number of lines originating from this transition in the emission spectrum equal to the number of lattice sites occupied by  $\text{Eu}^{3+}$ . As seen from **Fig. 4**, a weak emission is observed at 579 nm ( ${}^5\text{D}_0 \rightarrow {}^7\text{F}_0$ ) transition indicating that  $\text{Eu}^{3+}$  occupies one of the environments of  $C_n$ ,  $C_{nv}$  and  $C_s$  symmetry<sup>21</sup>.

The magnetic dipole transition  ${}^5\text{D}_0 \rightarrow {}^7\text{F}_1$  with a selection rule  $\Delta J = \pm 1$  is hardly affected by the crystal field strength around the  $\text{Eu}^{3+}$  ions because it is parity-allowed and dependent on the glass environment exhibiting an orange emission. From **Fig. 4** it is also observed that  $\text{Eu}^{3+}$  at 6-coordination environment shows a strong red emission at 613 nm ascribed to a forced electric dipole transition  ${}^5\text{D}_0 \rightarrow {}^7\text{F}_2$  with a selection rule  $\Delta J = \pm 2$ , which is a hypersensitive nature<sup>22,23</sup>. The transition  ${}^5\text{D}_0 \rightarrow {}^7\text{F}_3$  (652 nm) is strictly forbidden and possess low intensity due to J-mixing effect between multiplets and electric dipole transition  ${}^5\text{D}_0 \rightarrow {}^7\text{F}_4$  (701 nm) is also found to be of weak intensity.

The ligand field can split up  ${}^7\text{F}_j$  level into at most  $2J+1$  sublevels, depending on the symmetry around the ion. The intensities of the  ${}^5\text{D}_0 \rightarrow {}^7\text{F}_{j(=0, 1, 2, 3, 4)}$  transitions and splitting of the emission lines depends on the local symmetry of the crystal field of  $\text{Eu}^{3+}$ . If  $\text{Eu}^{3+}$  is embedded in the environment of inverse symmetry in the host matrix, optical transitions between the  $4f^6$  are strictly forbidden as electric dipole transitions ( ${}^5\text{D}_0 \rightarrow {}^7\text{F}_2$ ), the orange emission due to allowed magnetic dipole transitions  ${}^5\text{D}_0 \rightarrow {}^7\text{F}_1$  will be dominating transition, contrary to this, if  $\text{Eu}^{3+}$  occupies the non-inversion symmetry environment then electric dipole transitions are not strictly forbidden and  ${}^5\text{D}_0 \rightarrow {}^7\text{F}_2$  with a bright red emission is dominant at 613 nm. On comparing the intensity of emission peaks at 613 nm ( ${}^7\text{F}_2$  of ED) and 591 nm ( ${}^7\text{F}_1$  of MD) the luminescence originating from  ${}^7\text{F}_2$  is stronger than  ${}^7\text{F}_1$ , indicating that  $\text{Eu}^{3+}$  is located in a distorted (asymmetric) environment. The intensity ratio (R) between ED and MD transitions i.e. ( ${}^5\text{D}_0 \rightarrow {}^7\text{F}_2 / {}^5\text{D}_0 \rightarrow {}^7\text{F}_1$ ) is also known as asymmetry ratio, gives the distortion from inversion symmetry of the local environment around  $\text{Eu}^{3+}$  ions in the glass matrix is found to be 1.98. Larger the value of R, larger will be the magnitude of the electric dipole transition, high bond covalence and low ligand symmetry, which leads to stronger splitting of transitions. Smaller the value of R, more symmetry is the  $\text{Eu}^{3+}$  environment<sup>24</sup>. Intra- $4f$  electrons could occur via electric-dipole, magnetic-dipole transitions, electric quadrupole, vibronic transitions and phonon-assisted energy transfer arising from ion-ion coupling and multiphonon emission.

**Fig. 5** shows the energy level scheme of all the observed excitation and emission transitions of  $\text{Eu}^{3+}$ : BZM glass with 393 nm excitation. From the  ${}^5\text{D}_0$  level the  $\text{Eu}^{3+}$  ions decay radiatively, since the large energy difference of the  ${}^7\text{F}_6$  level presents the possibility of multiphonon relaxation as shown in the energy level scheme. **Fig. 6** presents the decay curve, which is plotted for the prominent emission transition  ${}^5\text{D}_0 \rightarrow {}^7\text{F}_2$  at 613 nm with an excitation wavelength of 393 nm. The decay curve exhibited an exponential nature and its lifetime has found to be 1.81 ms.

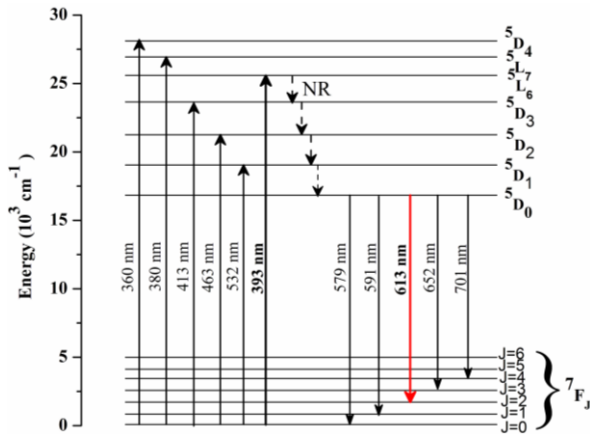


Fig. 5. Energy level scheme of all the observed excitation and mission transitions of  $\text{Eu}^{3+}$ :BZM glass

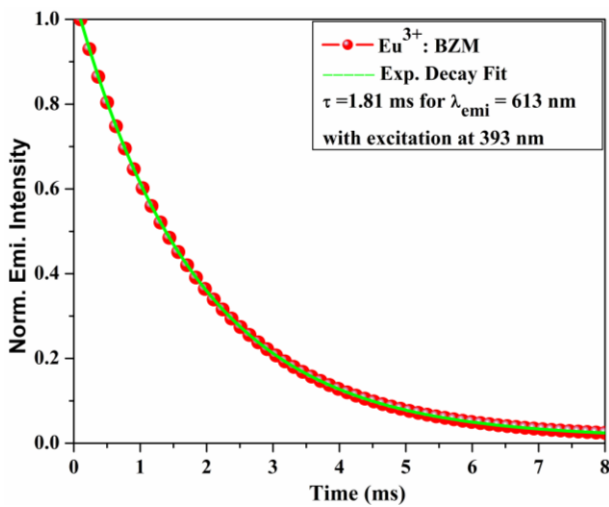


Fig. 6. Emission decay curve for emission transition of  $\text{Eu}^{3+}$ : BZM glass

#### 4. Conclusion

In summary, it could be concluded that we have successfully developed highly transparent, moisture resistant and stable (0.2 mol %)  $\text{Eu}^{3+}$  ions doped Borate Zinc Magnesium glasses. Optical analysis of these glasses has been carried out based on the measurement of the absorption, excitation and emission spectra. Up on exposure to UV rays, these glasses have shown *bright red* emission from their surfaces. We have plotted the decay curve in order to determine the emission life time.

#### References

1. Qiao, X., Fan, X., Wang, M., Adam, J. L., and Zhang, X., Spectroscopic properties of  $\text{Er}^{3+}/\text{Yb}^{3+}$  co-doped  $50\text{SiO}_2\text{-}20\text{Al}_2\text{O}_3\text{-}30\text{CaF}_2$  glass and glass ceramics, *J. Phys.: Condens. Matter*, 2006, 18, 6937–6951.
2. Lin, H., Yang, D., Liu, G., Ma, T., Zhai, B., An, Q., Yu, J., Wang, X., Liu, X., and Pun, E. Y. B., Optical absorption and photoluminescence in  $\text{Sm}^{3+}$  and  $\text{Eu}^{3+}$  doped rare-earth borate glasses, *J. Lumin.*, 2005, 113, 121–128.
3. Feng, X., Tanabe, S., and Hanada, T., Spectroscopic Properties and Thermal Stability of  $\text{Er}^{3+}$ -Doped Germanotellurite Glasses for Broadband Fiber Amplifiers, *J. Am. Ceram. Soc.*, 2001, 84, 165–171.
4. Lin, H., Pun, E. Y. B., Wang, X., and Liu, X., Intense visible fluorescence and energy transfer in  $\text{Dy}^{3+}$ ,  $\text{Tb}^{3+}$ ,  $\text{Sm}^{3+}$  and  $\text{Eu}^{3+}$  doped rare-earth borate glasses. *J. Alloys Compounds*. 2005, 390, 197–201.
5. Lin, H., Tanabe, S., Lin, L., Yang, D. L., Liu, K., Wong, W. H., Yu, J. Y., and Pun, E. Y. B., Infrequent blue and green emission transitions from  $\text{Eu}^{3+}$  in heavy metal tellurite glasses with low phonon energy. *Phys. Lett. A.*, 2006, 358, 474–477.

6. Kumar, A., Rai, D. K., and Rai, S. B., Optical studies of  $\text{Eu}^{3+}$  ions doped in tellurite glass. *Spectrochim. Acta A*, 2002, 58, 2115–2125.
7. Pisarski, W. A., Pisarska, J., Dominiak-Dzik, G., Maćzka, M., and Ryba-Romanowski, W., Compositional-dependent lead borate based glasses doped with  $\text{Eu}^{3+}$  ions: Synthesis and spectroscopic properties, *J. Phys. Chem. Solids*, 2006, 67, 2452–2457.
8. Pisarski, W. A., Pisarska, J., Maćzka, M., and Ryba-Romanowski, W., Europium-doped lead fluoroborate glasses: Structural, thermal and optical investigations, *J. Mol. Struct*, 2006, 792/793, 207–211.
9. Kam, C. H., and Buddhudu, S., Emission analysis of  $\text{Eu}^{3+}:\text{Bi}_2\text{O}_3\text{-B}_2\text{O}_3\text{-R}_2\text{O}$  ( $\text{R}=\text{Li, Na, K}$ ) glasses, *J. Quantum Spectrosc. Radiat. Trans*, 2004, 87, 325–337.
10. Chakrabarti, R., Das, M., Karmakar, B., Anapurna, K., and Buddhudu, S., Emission analysis of  $\text{Eu}^{3+}:\text{CaO-L}_2\text{O}_3\text{-B}_2\text{O}_3$  glass, *J. Non-Cryst. Solids*, 2007, 353, 1422–1426.
11. Nageno, Y., Takebe, H., Morinaga, K., and Izumitani, T., Effect of modifier ions on fluorescence and absorption of  $\text{Eu}^{3+}$  in alkali and alkaline earth silicate glasses, *J. Non-Cryst. Solids*, 1994, 169, 288–294.
12. McDougall, J., Hollis, D. B., and Payne, M. J. B., Judd-offelt parameters of Rare-earth ions in ZBLA fluoride glass, *Phys. Chem. Glasses*, 1994, 35, 258–259.
13. Balda, R., Fernandez, J., Adam, J. L., and Arriandiaga, M. A., Time-resolved fluorescence-line narrowing and energy-transfer studies in a  $\text{Eu}^{3+}$ -doped fluorophosphate glass, *Phys. Rev. B*, 1996, 54, 12076–12086.
14. Zhao, D., Qiao, X., Fan, X., and Wang, M., Local vibration around rare earth ions in  $\text{SiO}_2\text{-PbF}_2$  glass and glass ceramics using  $\text{Eu}^{3+}$  probe, *Physica B*, 2007, 395, 10–15.
15. Reisfeld, R., Radiative and non-radiative transitions of rare-earth in glasses, *struct. Bonding (Berlin)*, 1975, 22, 123–75.
16. Layne, C. B., and Weber, M. J., Multiphonon relaxation of rare-earth ions in beryllium-fluoride glass, *Phys. Rev. B*, 1977, 16, 3259–3261.
17. Thulasiramudu, A., and Buddhudu, S., Optical characterization of  $\text{Eu}^{3+}$  and  $\text{Tb}^{3+}$  ions doped zinc lead borate glasses, *Spectrochim. Acta A*, 2007, 66, 323–328.
18. Jamalajah, B. C., Suresh Kumar, J., Mohan Babu, A., and Rama Moorthy, L., Spectroscopic studies of  $\text{Eu}^{3+}$  ions in LBTAf glasses, *J. Alloys Compounds*, 2009, 478, 63–67.
19. Reisfeld, R., Greenberg, E., Brown, R. N., Drexhage, M. G., Jorgensen, C. K., Fluorescence of europium (III) in a fluoride glass containing zirconium, *J. Chem Phys. Lett.* 1983, 95, 91–95.
20. Kam, C. H., Buddhudu, S., Photoluminescence properties of  $\text{Eu}^{3+}:\text{ZrF}_4\text{-BaF}_2\text{-LaF}_3\text{-YF}_3\text{-AlF}_3\text{-NaF}$  glasses, *Physica B*, 2004, 344, 182–189.
21. Li, Z., Zeng, J., Zhang, G., Li, Y., A new promising Phosphor,  $\text{Na}_3\text{La}_2(\text{BO}_3)_3:\text{Ln}$  ( $\text{Ln}=\text{Eu, Tb}$ ), *J. Solid State Chem.* 2005, 178, 3624–3630.
22. Judd, B. R., Optical Absorption Intensities of Rare-Earth Ions, *Phys. Rev*, 1962, 127, 750–761.
23. Ofelt, G. S., Intensities of Crystal Spectra of Rare-Earth Ions, *J. Chem. Phys*, 1962, 37, 511–520.
24. Gallagher, P. K., Absorption and Fluorescence of Europium (III) in Aqueous Solutions, *J. Chem Phys*, 1964, 41, 3061–3069.

\*\*\*\*\*